Journal of Chemical and Petroleum Engineering (JChPE)

Print ISSN: 2423-673X Online ISSN: 2423-6721

The Effect of Carbonate Cement Type on Sandstone Matrix Acidizing

Hossein Younesian-Farid, Saeid Sadeghnejad *

1. Department of Petroleum Engineering, Faculty of Chemical Engineering, Tarbiat Modares University, Tehran, Iran. E-mail: hosseinunesian@modares.ac.ir
2. Department of Petroleum Engineering, Faculty of Chemical Engineering, Tarbiat Modares University, Tehran, Iran. E-mail: sadeghnejad@modares.ac.ir

ARTICLE INFO

Article History:
Received: 27 September 2021
Revised: 29 August 2022
Accepted: 29 August 2022

Article type: Research

Keywords:
Cement Dominant Reactions,
Dissolution Modelling,
Hydrochloric Acid,
Reactive Flow,
Sandstone Acidizing

ABSTRACT

This study aims to numerically determine the roles of the geochemical reactions during the injection of a strong acid into a sandstone sample. As a case study, we used laboratory results of hydrochloric acid (HCl) injection into a sandstone core plug sample from the literature. As the exact cement composition of the implemented sandstone was not available, two probable cement compositions were considered (i.e., calcite and dolomite cement). A fully-implicit model, coded in Python, was used to simulate the underlying geochemical reactions during the HCl injection (i.e., equilibrium and kinetical reactions). In addition, the reactive surface area and porosity-permeability changes of the rock sample were included in the model. The modeling results show that dolomite cement matched better than calcite cement with the experimental acidizing data. A perfect effluent pH prediction was therefore achieved when the reactive surface area was considered as a function of mineral volume fraction. Moreover, a detailed analysis of the dissolution/precipitation rate of different minerals involved in simulations was provided. The presented model improves our understanding of sandstone acidizing by determining dominant reactions.

Introduction

Predicting the behavior of an invading fluid in hydrocarbon reservoirs is of great importance. Among invading fluids, those that react with reservoir rocks or fluids (e.g., acidizing) are the most complex cases. Continuum-scale reactive transport models at the core scale are and will remain the only tools suitable for making long-term predictions of natural systems [1]. Identifying dominant reactions during an acidizing process in porous media is the key to success. These reactions vary based on injected acids and rock composition. Some reactions may have a negative impact on the acidizing process [2]. Even those reactions that contribute to rock dissolution should be controlled because an excessive amount of dissolution might result in an instability of rock structure [3]. Therefore, it is crucial to know the mechanisms of reactions, their thermodynamics, and kinetics.

Hydrocarbon reservoirs are generally divided into carbonate and sandstone formations. The former is commonly composed of calcite or dolomite, while the latter has more complex compositions. In carbonate acidizing, it is essential to control the operation to create stable wormholes [4, 5]. In sandstones, however, the main factor determining the efficiency of an

* Corresponding Author: S. Sadeghnejad (E-mail address: sadeghnejad@modares.ac.ir)

Journal of Chemical and Petroleum Engineering, 2022, 56(2): 245- 255.
Publisher: University of Tehran, College of Engineering *DOI: 10.22059/JCHPE.2022.331409.1363*

acidizing process is permeability increment by removing some minerals such as carbonate cement and clays and reducing the possibility of byproduct precipitation [6-8].

Choi [9] conducted an HCl injection into a sandstone core. They also proposed a three-mineral model approach (i.e., quartz, anorthite, and kaolinite) to simulate this process and provided an appropriate prediction of pH changes. However, their model failed to accurately predict the concentration of effluent species. Moreover, their study did not determine the exact composition of the sandstone core. Benson [10] considered a four-mineral model (i.e., quartz, kaolinite, calcite, K-feldspar) to simulate potential reactions during the experiment of Choi [9]. They used the GEM-GHG simulator that considers aqueous reactions to be locally in equilibrium. This simulator can calculate the rate of heterogeneous reactions using a general reaction-rate equation. Despite valuable progress compared to the model of Choi [9], the results of this model for the concentration of Ca^{2+}, Al^{3+}, and H_4SiO_4 (in some of the injection periods) were different than the experimental results. Kazempour and Alvarado [11] proposed another four-mineral model (i.e., quartz, kaolinite, dolomite, and K-feldspar) for predicting the composition of the same sandstone rock. They simulated the process of HCl injection by Geochemist's Workbench Professional (GWB). They assumed that quartz takes part in an equilibrium reaction while the other three minerals (i.e., dolomite, kaolinite, and K-feldspar) take part in kinetic reactions. Despite implementing various models to predict the behavior of acidizing in this sandstone sample, none of the aforementioned studies in the literature could predict the effluent concentrations precisely. The main uncertain parameter in this acid injection experiment, which was not considered, was the cement type. Cement type directly influences the geochemical reactions during acidizing in sandstones. Furthermore, a fixed value for the reactive surface area was only implemented in most of those models, while this parameter can be a function of mineral volume fractions and porosity during reactions.

In this study, the role and impact of cement composition on acidizing behavior of the sandstone sample are evaluated. We consider two different rock compositions with a four-mineral approach to investigate the behavior of dominant reactions during the acidizing of the sandstone sample. The experimental results of Choi [9] are used for comparison purposes. The HCl injection into the sandstone core is modeled via a fully implicit reactive flow model developed in Python. The porosity is updated based on the dissolution/precipitation rates of minerals, and the permeability is modified based on porosity changes. A modified equation is proposed for the evolution of the reactive surface area (RSA), and the reaction rate constants for each reaction are determined. In our new RSA model, the evolution of minerals during dissolution and precipitation is considered a function of mineral volume fractions and porosity, respectively. This is followed by a complete description of the minerals' temporal dissolution patterns and reaction rates.

Materials and methods

2.1. Statement of the Problem

In this study, HCl injection into a sandstone core plug sample is modeled. The dominant reactions are considered, and the concentration variation of species across the core is investigated. To evaluate our introduced model, we use the experimental data of Choi [9], who conducted an HCl injection into a sandstone rock sample. The experiment details are discussed in section 2.4. The pH and the concentration of four species (i.e., Ca^{2+}, Al^{3+}, K^{+}, and Si) were measured at the outlet of the core sample. Unfortunately, their study did not determine the exact composition of the sandstone core. Therefore, the proposed models for explaining the dominant reactions are mainly based on analyzing the concentration of the produced ions and pH changes.

This study considers two different compositions for the sandstone rock; the model I: 69.5% quartz, 2.5% K-feldspar, 5% kaolinite, and 5.3% calcite, and model II: 70.2% quartz, 2.5% K-feldspar, 5% kaolinite, and 4.6% dolomite. In the first model (model I), the sandstone carbonate cement is composed mostly of calcite (the same minerals were considered in Benson [10]). In contrast, the second model (model II) is mainly composed of dolomite. The HCl injection into both rock compositions is modeled and compared with the experimental data. The impact of dissolution on RSA is investigated as well (section 2.3). This study aims to quantitatively clarify the effect of the carbonate cement composition on the concentration of the produced ions. Moreover, we provide information regarding the changes in each mineral during the stimulation process.

2.2. Definition of Dominant Reactions

Determining the slow and fast-reacting minerals and their reaction rates is crucial to investigate the structural changes of porous media during acidizing. These reactions determine the acid consumption rate and affect minerals' dissolution patterns. Table 1 represents the conventional reactions of the available minerals in the sandstone rock during HCl injection. These reactions indicate the interaction of aqueous species with the available rock minerals.

Table 1. Considered reactions during HCl injection into the sandstone core

	No.	Minerals	Dissolution/Precipitation Reactions of Minerals	Log(K_{eq}) [12, 13]
The involved reactions in both models	(1)	Quartz	$SiO_{2(S)} + 2H_2O \rightleftharpoons H_4SiO_4$	-3.98
	(2)	K-feldspar	$KAlSi_3O_{8(S)} + 8H_2O \rightleftharpoons K^+ + Al(OH)_4^- + 3H_4SiO_4$	-20.57
	(3)	Kaolinite	$Al_2Si_2O_5(OH)_{4(S)} + 6H^+ \rightleftharpoons 2Al^{3+} + 2H_4SiO_4 + H_2O$	7.43
Considered in model 1	(4)	Calcite	$CaCO_{3(S)} + H^+ \rightleftharpoons Ca^{2+} + HCO_3^-$	1.85
Considered in model 2	(5)	Dolomite	$CaMg(CO_3)_{2(S)} + 2H^+ \rightleftharpoons Ca^{2+} + Mg^{2+} + 2HCO_3^-$	3.53

The main homogeneous reactions (reactions inside the aqueous phase) are presented in Table 2. The homogeneous reactions have a high rate and are considered to achieve an instantaneous equilibrium at any moment (i.e., time step) [14, 15].

Table 2. Equilibrium reactions in the aqueous phase

Equilibrium Reactions	Log(K_{eq}) [12, 13]
$Al(OH)_4^- + 4H^+ \rightleftharpoons Al^{3+} + 4H_2O$	22.70
$CO_3^{2-} + H^+ \rightleftharpoons HCO_3^-$	10.33
$CaOH^+ + H^+ \rightleftharpoons Ca^{2+} + H_2O$	12.78
$Ca(HCO_3)^+ \rightleftharpoons HCO_3^- + Ca^{2+}$	-1.10
$OH^- + H^+ \rightleftharpoons H_2O$	14.00
$CaCl_2 \rightleftharpoons Ca^{2+} + 2Cl^-$	0.64
$HCl \rightleftharpoons H^+ + Cl^-$	0.71

Table 3 summarizes the forward reaction rate constants and the initial RSA of the minerals in both models.

Table 3. Forward reaction rate constants and the initial RSA of the minerals

No.	Mineral	Forward Reaction Rate Constant (k_f)	Initial Reactive Surface Area $A_{S,0}$ (m^2/ m^3)	
			Model I	Model II
1	Quartz	-6.32	695,000	702,000
2	K-feldspar	-6.72	25,000	25,000
3	Kaolinite	-7.43	50,000	50,000
4	Calcite	-1.27	53,000	--
5	Dolomite	-1.67	--	46,000

$A_{s,0}$ of each mineral is calculated as a function of the initial volume fraction of that mineral ($A_{s,0} = V_{s,0} \times 10^6$).

2.3. Numerical Model Formulation

Eqs. 1 and 2 show the main transport equations of the system. Eq. 1 originated by considering the mass balance for a slightly compressible fluid flow. The second transport equation is written for the convective-diffusive transport of species in the system. This equation is acquired by writing the mass balance for the primary and secondary species [15]. This final format needs to be solved just for the primary species. The concentration of the secondary species is calculated by exploiting the mass action law equation.

$$\frac{\partial(\rho u_x)}{\partial x} = \rho\varphi\,(C_l + C_r)\frac{\partial(P)}{\partial t} \tag{1}$$

$$\frac{\partial(u_x(C_j + \sum_{i=1}^{N_x} v_{ij}X_i))}{\partial x} - D\frac{\partial^2(C_j + \sum_{i=1}^{N_x} v_{ij}X_i)}{\partial x^2} + \frac{\partial(\varphi(C_j + \sum_{i=1}^{N_x} v_{ij}X_i))}{\partial t} + R_j^{\min} + \sum_{i=1}^{N_x} v_{ij}R_i^{\min} = 0 \tag{2}$$

in Eqs. 1 and 2, ρ and C_l are the fluid density and compressibility; N_x is the number of the selected secondary species (X_i), φ and C_r represent the porosity and the compressibility of the rock; v_{ij} is the stoichiometric coefficient of the primary species of j divided by that of the secondary species of i in an aqueous reaction; P and u_x indicate the pressure and velocity of the fluid; and R_j^{min} as well as R_i^{min} are the reaction rates of the primary and secondary species in heterogeneous reactions. By developing our model in Python, Eqs. 1 and 2 are simultaneously solved for all of the primary species that are available in the system.

A specified concentration of acid (HCl) is injected into a core from the left boundary at a constant rate. C_{inj} is the concentration of the injected components, u_{inj} is the inlet velocity of the fluid, and P_{atm} is the atmospheric pressure. The considered number of grid points is 50 in our study, which is determined by sensitivity analysis. As it is specified in Eqs. 1 and 2, the pressure of the grid blocks and the concentration of the species are the main unknown parameters. The unknowns of the nonlinear partial differential equations are solved fully implicitly by implementing the Newton-Raphson method. More information concerning the details of the modeling approach can be found elsewhere [16, 17].

The RSA of a mineral (i.e., the part of a mineral surface that is exposed to a reaction) changes with the progress of the reaction [18]. This can be originated either from the evolution of a mineral structure during the dissolution or from covering the surface of a mineral during the precipitation process. Using Eqs. 3 and 4 in our model, it is assumed that the RSA is a function of mineral volume fraction during the dissolution and porosity during the precipitation process.

$$A_{dissolution} = A_{m,0}\left(\frac{V_m}{V_{m,0}}\right)^2 \tag{3}$$

$$A_{precipitation} = A_{m,0}\left(\frac{\varphi}{\varphi_0}\right)^2 \tag{4}$$

where, $A_{m,0}$ is the initial RSA of minerals and V_m is their volume fraction, and φ is the porosity of the system. The primary form of these two equations can be found elsewhere [19]. In our modeling approach, we used these modified forms (i.e., Eqs. 3 and 4) to receive a better match with the experimental results. $A_{m,0}$ of each mineral can be considered to be a function of the

volume fraction of that mineral ($A_{m,0} = V_{m,0} \times (10^4 or 10^6)$) according to [10]). These values are presented in Table 3.

Different reaction rate models were defined for heterogeneous reactions (i.e., the reactions in Table 1) of our model. From each homogeneous reaction in Table 2, one species was selected as the secondary species, and its concentration was calculated by mass action law. This approach results in fewer unknown parameters and increases the simulation speed [15]. Except for the dolomite dissolution, we used the stoichiometric coefficients as the order of reactions concerning each species. The forward reaction rate of dolomite dissolution was considered a function of the H^+ concentration.

The simulation starts with reading input data such as fluid and rock properties and the stoichiometric coefficients of reactions. Then, the pressure distribution and ions concentration are computed by applying the Newton-Raphson method. A variable time step is considered, and it is updated during simulations. It is always kept lower than the maximum value defined by the user. Whenever any convergency problem occurs, the time step is automatically decreased. At the next simulation step, the volume fraction of minerals and porosity of all grid blocks are explicitly updated. This process continues until the final simulation time reaches.

2.4. Experiment Details

During the injection process [9], HCl was injected into a sandstone core at a constant rate (Q=2 cc/minute). The length of the core was 22.47 cm, and its diameter was 2.49 cm. The initial porosity and permeability were measured at 0.177 and 56 md, respectively. At the first step, an 11 PV of 3% wt NaCl solution was injected into the core until a stable pressure drop was achieved. The purpose of this NaCl injection was to measure the permeability of the core sample. Afterward, a 259 PV of the HCl solution with an initial pH of 1 (C_{HCl} = 0.1 Molar) was injected. There were also several shuts-in during the injection of this acidizing process. The pH of the fluid that had left the core (effluent) was recorded versus time. The concentration of the four species of Si, Al^{3+}, Ca^{2+} and K^+ in this fluid was measured by the inductively coupled plasma (ICP) method at different time intervals.

Results and Discussion

3.1. Prediction of Effluent Species

In this study, the impact of the rock composition on the dissolution process is quantitatively investigated. The uncertain parameters are found in a way that acceptable results are obtained. Fig. 1 compares the results of cement-type models I and II with the concentration of Al^{3+}, H_4SiO_4, and K^+ from the acidizing experiment. Comparing the predictions of the model with different cement types (Model I and II) with the experimental data demonstrates that both models provide a good forecast for the concentration of Al^{3+}, H_4SiO_4, and K^+. Moreover, the predictions are not sensitive to the cement composition.

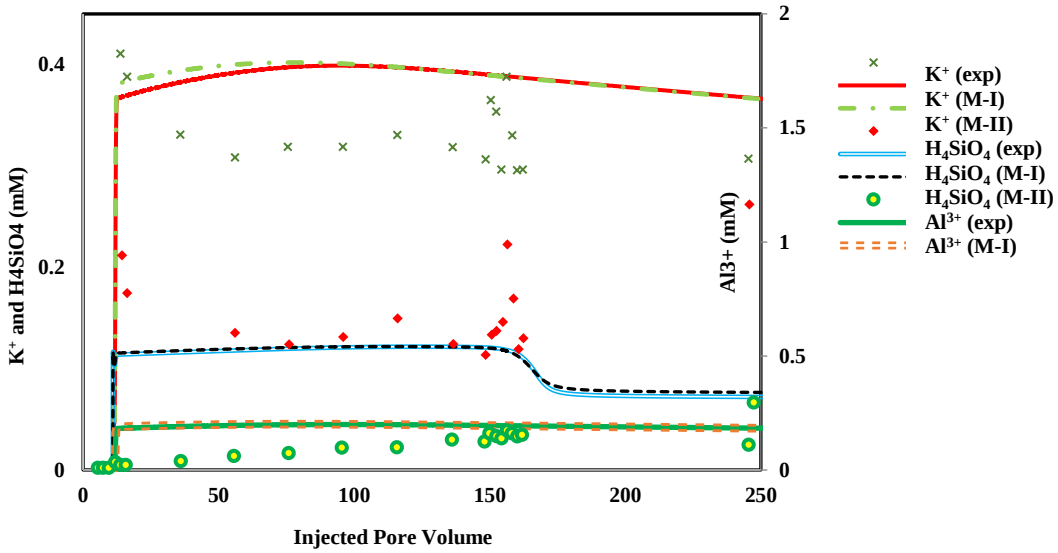

Fig. 1. Comparison of the modelling results with the experimental data for the concentration of different species, considering two other models for the cement composition of the sandstone core (M-I and M-II represent Model I and II, respectively)

K-feldspar is the only source of K^+, and the dissolution of this mineral results in the production of this ion (the second reaction in Table 1). Therefore, finding the reaction rate constant of K-feldspar (based on the concentration of K^+) is straightforward. However, the concentration of the other two species (i.e., Al^{3+} and H_4SiO_4) does not depend on a single mineral. The dissolution of K-feldspar and kaolinite can affect the concentration of Al^{3+} (by producing Al^{3+}) and $Al(OH_4)^-$, respectively (the second and third reactions in Table 1**Error! Reference source not found.**). In the same way, the concentration of H_4SiO_4 depends on the reactions of three minerals of quartz, K-feldspar, and kaolinite (the first through third reactions in Table 1**Error! Reference source not found.**). Therefore, finding the reaction rate constant of these three minerals is a more challenging task. According to Fig. 1, the cement composition of Models I and II provides similar results for the concentration of Al^{3+}, H_4SiO_4, and K^+. The type of carbonate cement (calcite and dolomite) differs in these two models. According to the reactions of 4 and 5 in Table 1, the dissolution of calcite or dolomite does not directly produce any of these three species. Therefore, the predictions of both models for the concentration of these three species are very similar.

Fig. 2 compares the prediction of both cement models (i.e., Model I and II) with the experimental data. Moreover, we have compared our prediction with the results of former simulations in the literature (i.e., Benson [10] and Kazempour and Alvarado [11]) for the concentration of calcium ions. According to this figure, assuming dolomite (i.e., Model II) rather than calcite (i.e., Model I) as the carbonate cement results in a more truthful prediction [Ca^{2+}]. The prediction of our second model (Model II) for the concentration of this ion is more accurate than the results of other published simulations presented in this figure. According to the stoichiometry of the fourth reaction in Table 1, if one mole is consumed with calcite, one mole of Ca^{2+} is produced. However, two moles of H^+ are required to produce the same amount of Ca^{2+} from a dolomite dissolution (the fifth reaction in Table 1),. This procedure explains the lower amounts of Ca^{2+} production when the dolomite cement composition is considered. Thus, the output results of this model are closer to the experimental results.

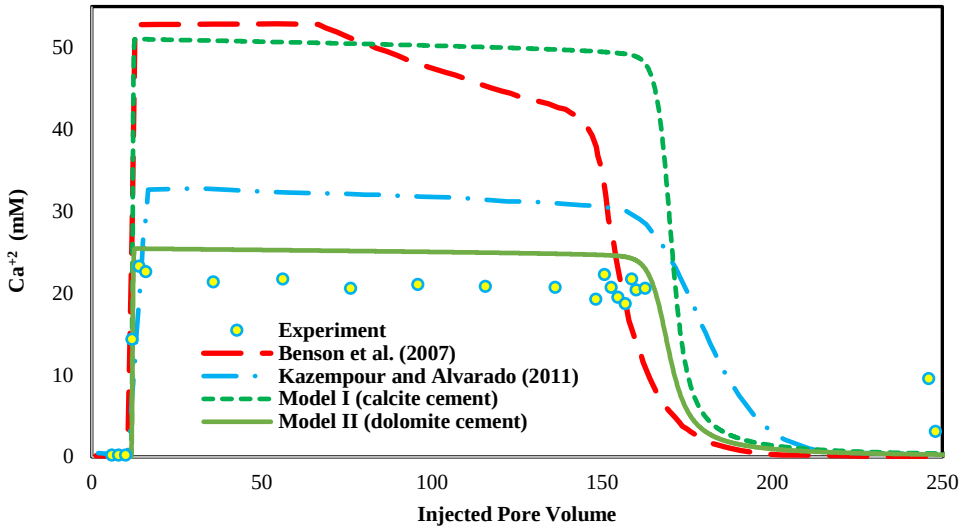

Fig. 2. Comparing the results of our models (i.e., Model I and II) with the experimental data and former simulations in the literature (i.e., Benson [10] and Kazempour and Alvarado [11]) for the concentration of calcium ion

3.2. Prediction of the Outlet pH

Fig. 3 indicates the simulation results and the experimental data for the pH of effluents. The effluent pH slightly decreases until almost 140 PV injections of the HCl solution. This is because of the calcite/dolomite dissolution and a decrease in their volume fraction. According to Eq. 4, the RSA of the forward reaction is considered to be a function of the second power of the volume fraction of the minerals. Therefore, the RSA of calcite/dolomite decreases by its dissolution. Thus, the amount of unreacted H^+ increases in the effluent, and the outlet pH slightly decreases. By using the primary form of Eq. 3, in which the RSA of the mineral dissolution was a function of both porosity and the volume fraction of that mineral, the effluent pH of the system did not show a decreasing trend in this injection period (i.e., injected pore volume < 140) and deviated from the experimental values. Therefore, this refined form of RSA (i.e., Eq. 3) is more acceptable during this period. When there is no calcite/dolomite left in the core (injected pore volume of acid > 170 in Fig. 3), the effluent pH approaches close to that of the injected solution (i.e., the effluent pH decreases to 1).

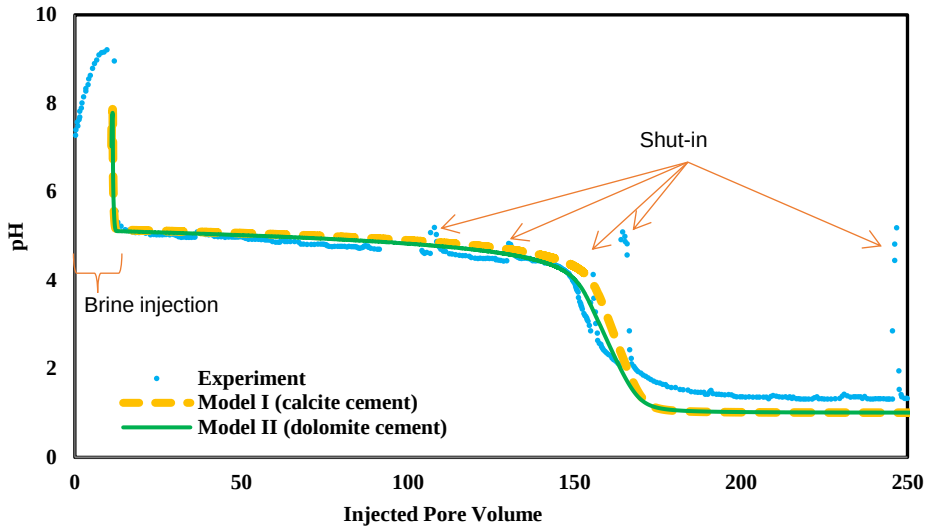

Fig. 3. Comparison of the simulation results with the experimental data for the pH of the outlet fluid, considering two different models for the composition of the sandstone core

3.3. Analyzing the Dissolution Behaviour of Rock Constitutes

It was considered that the heterogeneous reactions (listed in Table 1) are reversible. The concentration of the involved species in a reaction determines the net rate of that reaction, which can be positive (for dissolution) or negative (for precipitation). Fig. 4 shows the reaction rate of minerals and their volume fractions along the core during the entire period of acid injection. The x-axis indicates the core length, and the y-axis represents the pore volume number of the acid solution injected into the core. In other words, the y-axis can be representative of time.

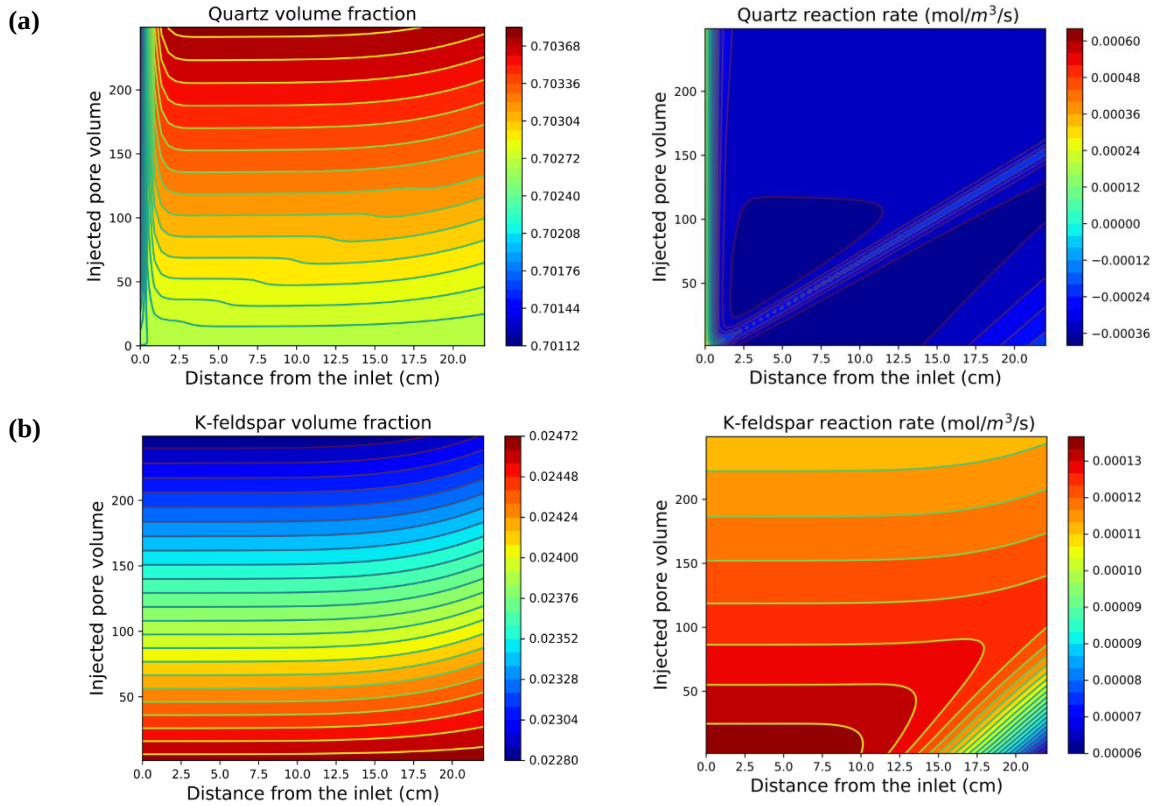

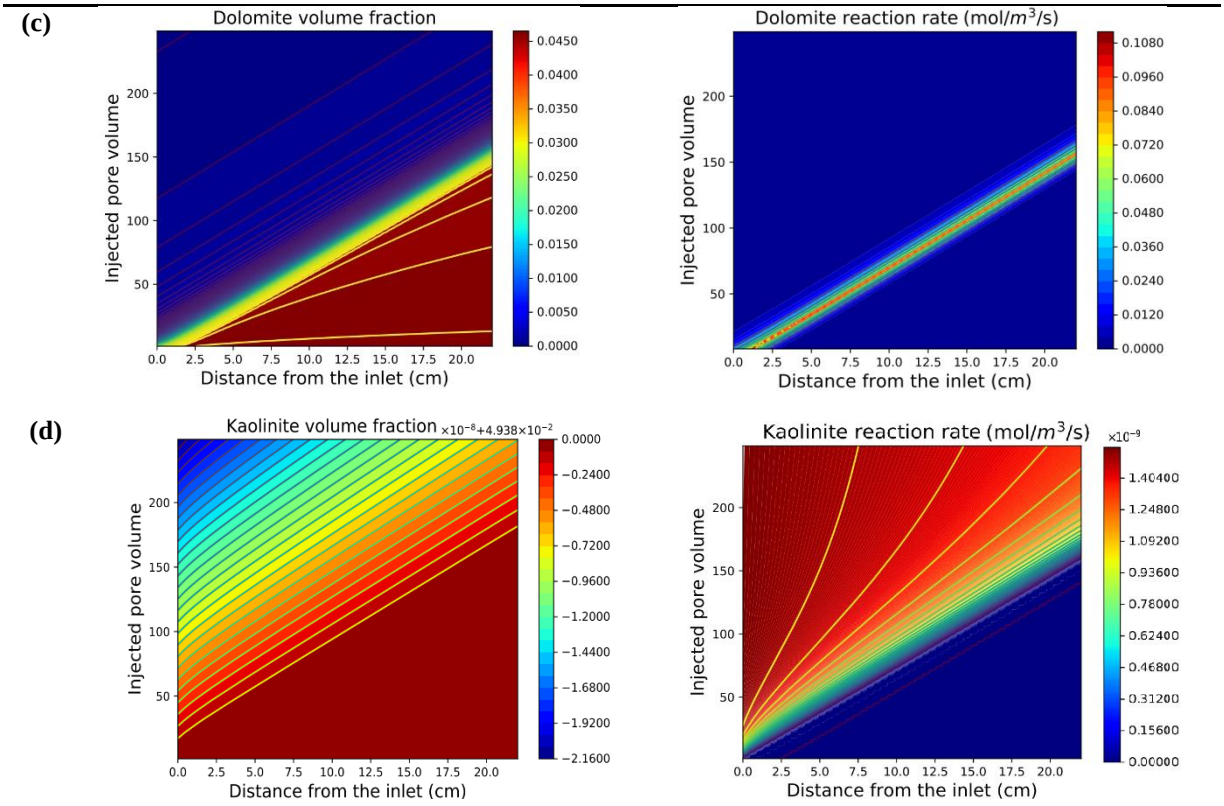

Fig. 4. The volume fraction (left) and the reaction rate (right) of the four minerals across the core versus the pore volume of the injected acid. (a) Quartz; (b) K-feldspar; (c) Dolomite; (d) Kaolinite

According to Fig. 4, the minerals have experienced different evolution ways. Fig. 4a indicates that quartz undergoes dissolutions in the areas near the inlet face (distance from the inlet < 1 cm). However, at the downstream parts of the core, the volume fraction of this mineral increases because of its precipitation. This precipitation originates from excessive H_4SiO_4 in the solution produced during K-feldspar dissolution (the second reaction in Table 1). The precipitation of quartz was also observed in simulations conducted by Choi [9] when they assumed the three minerals of anorthite, kaolinite, and quartz as the core components.

K-feldspar has experienced a uniform dissolution (Fig. 4b). The reaction rate of this mineral at all grid blocks is almost equal, resulting in a uniform distribution of this mineral across the core in each time step. According to Fig. 4c, dolomite dissolution follows a face dissolution regime. When the volume fraction of this mineral approaches zero in one grid, H^+ ions move toward the downstream sections. Otherwise, they are consumed in reactions with dolomite in that grid, and no considerable amount enters the core's downstream areas. This dissolution regime originated from the high reaction rate of dolomite in contact with the HCl solution. The reaction rate of dolomite in Fig. 4c has approached zero in all sections of the core after almost 170 PV injections of the HCl solution, which confirms that there is no dolomite left in the rock for further dissolution.

Kaolinite (Fig. 4d) has experienced the lowest change compared to the other three minerals. Its volume fraction slightly decreases over time. At the end of injection, the areas near the inlet have a lower volume fraction of kaolinite in comparison with the downstream sections of the core. This mineral is not the only source of Al^{3+}. The main part of Al^{3+} is produced from the dissociation of the complex of $Al(OH_4)^-$ that was generated during the dissolution of K-feldspar.

Conclusion

This study highlights the impact of initial cement composition on simulation results of sandstone matrix acidizing with hydrochloric acid. It is assumed that the sandstone sample was composed of four minerals (i.e., quartz, anorthite, kaolinite, and carbonate cement), and two carbonate cement composition models were considered for the core sample. The difference between these two models is in the type of carbonate cement (i.e., Model I: calcite cement, Model II: dolomite cement). The results are as follows,

- Considering dolomite as the carbonate cement of the core resulted in achieving an excellent agreement between the simulation results and the experimental data.
- HCl completely dissolved the dolomite cement inside of the rock. Moreover, K-feldspar underwent a uniform dissolution but in much smaller quantities. Furthermore, kaolinite (slow-reacting mineral) experienced a slight dissolution.
- Quartz experienced both dissolution and precipitation. It was dissolved at upstream core sections and precipitated at downstream areas. The reason was the generation of excessive values of H_4SiO_4 in the solution (because of K-feldspar dissolution) that derived the quartz reaction in the backward direction.

The forward reaction rate of dolomite is directly related to the second power of the dolomite volume fraction, and it was independent of the system porosity. This assumption resulted in a better match with the experimental outlet pH data.

Nomenclature

$A_{S,0}$	Initial reactive surface area (m^2/ m^3)
ICP	Inductively coupled plasma
k_f	Forward reaction rate constant
P	Pressure
Q	injection rate
RSA	reactive surface area
R_j^{min}	reaction rates of the primary species
R_i^{min}	reaction rates of the secondary species
u_x	velocity of the fluid
V_m	volume fraction of minerals
φ	porosity
v_{ij}	stoichiometric coefficient of the primary species of j divided by that of the secondary species of i

References

[1] Sadeghnejad S, Enzmann F, Kersten M. Digital rock physics, chemistry, and biology: challenges and prospects of pore-scale modelling approach. Applied Geochemistry. 2021;131:105028.

[2] Khojastehmehr M, Bazargan M. A new geochemical reactive transport model for sandstone acidizing. Computers & Geosciences. 2022;166:105178.

[3] 3.Hou B, Qui K, Chen M, Jin Y, Chen K. The wellbore collapse on sandstone formation during well test with matrix acidizing treatment. Petroleum science and technology. 2013;31(3):237-49.

[4] Li X, Gomaa A, Nino-Penaloza A, Chaudhary S, editors. Integrated Carbonate Matrix Acidizing Model for Optimal Treatment Design and Distribution in Long Horizontal Wells. SPE Production and Operations Symposium; 2015: Society of Petroleum Engineers.

[5] Dong R, Wang Q, Wheeler MF, editors. Prediction of mechanical stability of acidizing-induced wormholes through coupled hydro-chemo-mechanical simulation. 53rd US Rock Mechanics/Geomechanics Symposium; 2019: OnePetro.

[6] Shafiq MU, Mahmud HB. Sandstone matrix acidizing knowledge and future development. Journal of Petroleum Exploration and Production Technology. 2017;7(4):1205-16.

[7] Elakneswaran Y, Takeya M, Ubaidah A, Shimokawara M, Okano H, Nawa T, editors. Integrated geochemical modelling of low salinity waterflooding for enhanced oil recovery in carbonate reservoir. International Petroleum Technology Conference; 2020: OnePetro.

[8] Khurshid I, Al-Shalabi EW, Afgan I, Al-Attar H. A numerical approach to investigate the impact of acid-asphaltene sludge formation on wormholing during carbonate acidizing. Journal of Energy Resources Technology. 2022;144(6).

[9] Choi SK, Ermel YM, Bryant SL, Huh C, Sharma MM, editors. Transport of a pH-sensitive polymer in porous media for novel mobility-control applications. SPE/DOE Symposium on Improved Oil Recovery; 2006: Society of Petroleum Engineers.

[10] Benson IP, Nghiem LX, Bryant SL, Huh C, editors. Development and use of a simulation model for mobility/conformance control using a pH-sensitive polymer. SPE Annual Technical Conference and Exhibition; 2007: Society of Petroleum Engineers.

[11] Kazempour M, Alvarado V. Geochemically based modeling of ph-sensitive polymer injection in berea sandstone. Energy & Fuels. 2011;25(9):4024-35.

[12] Blanc P, Lassin A, Piantone P, Azaroual M, Jacquemet N, Fabbri A, et al. Thermoddem: A geochemical database focused on low temperature water/rock interactions and waste materials. Applied Geochemistry. 2012;27(10):2107-16.

[13] Parkhurst DL, Appelo C. Description of input and examples for PHREEQC version 3: a computer program for speciation, batch-reaction, one-dimensional transport, and inverse geochemical calculations. US Geological Survey; 2013. Report No.: 2328-7055.

[14] Balashov VN, Guthrie GD, Hakala JA, Lopano CL, Rimstidt JD, Brantley SL. Predictive modeling of CO2 sequestration in deep saline sandstone reservoirs: Impacts of geochemical kinetics. Applied Geochemistry. 2013;30:41-56.

[15] Steefel C, Appelo C, Arora B, Jacques D, Kalbacher T, Kolditz O, et al. Reactive transport codes for subsurface environmental simulation. Computational Geosciences. 2015;19(3):445-78.

[16] Younesian-Farid H, Sadeghnejad S. Geochemical performance evaluation of pre-flushing of weak and strong acids during pH-triggered polymer flooding. Journal of Petroleum Science and Engineering. 2019;174:1022-33.

[17] Koochakzadeh A, Younesian-Farid H, Sadeghnejad S. Acid pre-flushing evaluation before pH-sensitive microgel treatment in carbonate reservoirs: Experimental and numerical approach. Fuel. 2021;297:120670.

[18] Altree-Williams A, Brugger J, Pring A, Bedrikovetsky P. Coupled reactive flow and dissolution with changing reactive surface and porosity. Chemical Engineering Science. 2019;206:289-304.

[19] Steefel CI. CrunchFlow. Softw. Model. Multicomponent React. Flow Transp. User's Man. . Lawrence Berkeley Natl Lab, Berkeley USA. 2009.

How to cite: Younesian-Farid H, Sadeghnejad S. The Effect of Carbonate Cement Type on Sandstone Matrix Acidizing. Journal of Chemical and Petroleum Engineering. 2022; 56(2): 245-255.